APPLIED MICROBIAL AND CELL PHYSIOLOGY

Detoxification of Cu(II) by the red yeast *Rhodotorula mucilaginosa*: from extracellular to intracellular

Mengxiao Wang[1] · Jingxuan Ma[1] · Xuewei Wang[1] · Zhijun Wang[1] · Lingyi Tang[1] · Haoming Chen[1,2] · Zhen Li[1,3]

Abstract

The red yeast (*Rhodotorula mucilaginosa*: Rho) has abundant extracellular polymeric substances (EPS) and intracellular vesicles (Ves). This study explored the mechanisms of Rho to resist Cu toxicity from extracellular to intracellular, i.e., EPS, membrane, and Ves. The Cu^{2+} concentrations were set from 0 to 200 mg/L. In contrast to other heavy metals (e.g., Pb^{2+}), low Cu^{2+} stress has no evident stimulation to EPS production. In particular, GSH content in EPS did not show significant changes. The Cu removal was decreased from ~35 to ~0% as Cu stress raised from 0 to 200 mg/L, which confirmed the low binding of Cu cations to EPS. Moreover, redox peaks at -0.35 V (reduction) and -0.02 V (oxidation) in EPS were observed based on electrochemical analysis. Subsequently, the potential Haber-Weiss reaction in EPS lowered fungal ability to shield against the Cu toxicity. Then, the contrast of Cu concentration between the extracellular and intracellular regions was enlarged. Moreover, the thickness of cell membrane decreased from 450 to 116 nm during the elevation of Cu stress. These accelerated the transport of Cu cations into intracellular, but the redox reaction in both cell membrane and intracellular region was limited. Under transmission electron microscopy, the intracellular Ves showed evident sorption of Cu cations (100 mg/L). However, the Ves started to deform and gradually lost their activity at 200 mg/L. Therefore, this study successfully elucidated the correlated extracellular and intracellular mechanisms of metal detoxification by yeast.

Key points

•*This study provides a comprehensive explanation for the invasion of Cu^{2+} into fungal (Rhodotorula mucilaginosa) cells based on microbial physiological and biochemical analysis, electrochemical analysis, and transmitted electron microscopy.*
•*Cu nanoparticles are involved in redox reactions in the EPS, thus greatly reducing the prophase protection for fungal cells by EPS.*
•*At 200 mg/L Cu^{2+} stress, deformation of cell membrane intensifies the contrast of Cu concentrations between extra- and intracellular regions. This further suppresses the transportation of Cu^{2+} by intracellular vesicles.*

Mengxiao Wang, Jingxuan Ma and Xuewei Wang contributed equally to this work.

✉ Haoming Chen
  chenhaoming@njust.edu.cn

✉ Zhen Li
  lizhen@njau.edu.cn

[1] College of Resources and Environmental Sciences, Nanjing Agricultural University, Nanjing 210095, Jiangsu, China

[2] School of Environmental and Biological Engineering, Nanjing University of Science and Technology, Nanjing 210094, China

[3] Jiangsu Provincial Key Lab for Organic Solid Waste Utilization, Nanjing Agricultural University, Nanjing 210095, China

Introduction

Copper (Cu) is a trace element for living things. However, the excessive use of Cu has been causing global pollution due to the rising human activities such as mining, industrial processing, and utilization of pesticide and chemical fertilizers (Kaplan 1999; Wei et al. 2017). Cu pollution also causes serious economic losses (Sakhaee and Kazeminia 2011), e.g., hindering the survival and development of fry (Gouva 2020) and damaging lipids, proteins, and DNA of crops (Rehman et al. 2019). In addition, Wilson's, Alzheimer's, and Parkinson's diseases are all related to the imbalance of Cu

homeostasis (Bulcke et al. 2015). Therefore, Cu pollution requires our great attention.

Oversupply of Cu^{2+} partially disrupts the homeostasis balance between reactive oxygen species and antioxidant substances within the cells (Kan et al. 2019). It causes protein damage and lipid peroxidation, under either aerobic or anaerobic conditions. Microorganisms can survive from metal toxicity via their specific resistance systems (Silver and Walderhaug 1992). Their tolerance to heavy metals is critical to the successes of bioremediation (Tian et al. 2020). Extracellular polymeric substances (EPS) play an important role in helping microorganism to resist heavy metal stress outside of the cell, primarily via sorption and chelation (Kenney and Fein 2011). Intracellular stability of cells is regulated via a variety of metabolic pathways (e.g., tricarboxylic acid cycle, glycolysis pathway). For example, bacteria have evolved various mechanisms encoded by either chromosomal or plasmid genes via reducing Cu transport and enhancing efflux of Cu (Cervantes and Gutierrezcorona 1994). In addition, the presence of membranes complicates the homeostasis mechanism of heavy metals in bacteria, e.g., cytoplasmic membrane, cell membrane, and periplasmic space (Bondarczuk and Piotrowska-Seget 2013; Solioz et al. 2010). In particular, it was proposed that cell membrane contributes significantly to the adsorption of Cu^{2+} (Eisses et al. 2005). Similar to bacteria, cell wall and membrane in fungi also help to shield against Cu toxicity (Ramsay and Gadd 1997).

Red yeast *Rhodotorula mucilaginosa* is able to tolerate 200 mM Cu^{2+} and 500 mM Pb^{2+} (Kan et al. 2019). *Saccharomyces cerevisiae* removes 37% of the Cu^{2+} within 3 h (Gorobets et al. 2004). The carboxyl and amino groups in the cell wall of fungi contribute substantially to the sorption of Cu (Gorobets et al. 2004; Pearce and Sherman 1999; Wang 2002). It was proposed that superoxide dismutase or maroon can affect the tolerance of fungal cells to Cu^{2+} (Cervantes and Gutierrezcorona 1994; Kan et al. 2019). Vesicles (Ves) contain a variety of proteins, organic acids, organic bases, and other substances, which are capable of binding heavy metals (Liu et al. 2014b). As an important transport carrier in cells, Ves are able to transport toxic metals from intracellular to extracellular (Miyayama et al. 2009). However, the function of Ves in Cu detoxification has not been fully elucidated.

EPS have high heavy metal tolerance and strong adsorption capacity, which are usually considered the first "battle line" to shield against heavy metal toxicity. They have a greater binding capacity for metals than any currently known mineral sorbents (Quigley et al. 2002). Proteins in EPS exhibit a relatively high adsorption capacity for cations, followed by nucleic acid, and the least for polysaccharides (Wei et al. 2017). Additionally, the redox-active groups in EPS can interact with metal cations, causing electron transfer among the ions (Harish et al. 2012). The variety of biochemical

components causes various pathways of heavy metal fixation. For example, P species within EPS can bond with Cu^{2+} at a low level (0–2.5 mg/L) (Wang et al. 2015). Glutathione (GSH) can reduce the valence state of heavy metals (Yadav 2010) and form complex with various heavy metals (Podanyi and Reid 1988), which was usually considered as a high efficient component to reduce heavy metal toxicity (Li et al. 2019).

The objective of this study was to investigate the detoxification of Cu^{2+} by the red yeast *Rhodotorula mucilaginosa* (Rho), via extracellular and intracellular pathways. Rho with a high ability to produce abundant EPS was incubated under various Cu^{2+} stress from 0 to 200 mg/L. The adsorption capacity, microbial physiology, and cell morphology of Rho were investigated.

Materials and methods

Collection and incubation of Rho

The Rho strain was isolated from orchard rhizosphere soil and registered at China General Microbiological Culture Collection (CGMCC) as No. 16597. Rho was pre-cultured in potato glucose broth (PDB) medium. The broths were incubated at 28 °C on an orbital shaker at 180 rpm.

The Cu^{2+} concentrations were adjusted to 0, 50, 100, and 200 mg/L respectively, prepared by adding $CuSO_4 \cdot 5H_2O$ powder (Xilong Scientific Ltd.) into pure water. Then, 1-mL Rho suspension and 100-mL PDB medium were accordingly added to 250 mL Erlenmeyer flasks for incubation. All the treatments were then shaken at a rate of 180 rpm at 28 °C for 72 h with four replicates. After incubation, the sample bacterial liquid was separated to three parts following our previous protocol (Jiang et al. 2020b).

Cell count

1 mL of bacterial liquid was taken and counted in the blood cell counting chamber under light microscope, and the total bacterial number in 100 mL of bacterial liquid was calculated under an Olympus BX53 microscope (Olympus Corporation, Tokyo, Japan) with an Olympus LC30 camera (Olympus Soft Imaging Systems, Munster, German) and an oily lens (MSPlan × 100 objective lens).

ICP analysis

Bacterial liquid (35 mL) was centrifuged at 2743*g* for 3 min. The centrifuged supernatant was filtered with a 0.22-μm membrane for analysis by inductively coupled plasma (ICP). The concentration of Cu^{2+} in the supernatant was determined by an inductively coupled plasma optic emission spectrometry

(ICP-OES) instrument (Agilent 710, Agilent Technologies, USA). Calibration curve of Cu^{2+} (1, 2.5, 5, 10, 20 mg/L) was prepared.

TEM analysis

Partial precipitates after centrifugation were fixed using glutaraldehyde with a volume fraction of 2.5% and stored at 4 °C. Then, 60–80-nm unstained sections for transmission electron microscopy (TEM) were cut with a diamond knife on an Ultramicropore Leica EM UC7 slicer (Daitonme, Ultra 45°). To acquire the high-quality TEM images, a set of sections were stained with uranyl acetate and lead citrate. TEM was performed by the Hitachi HT7700 system (for stained section) and the FEI Tecnai G2 F20 TEM system (for unstained sections).

EPS extraction

The remaining 60-mL medium was collected for EPS extraction. Rho incubated for 3 days was centrifuged at a high speed (12,000g, 20 min) at 4 °C, followed by centrifugation (17,000g, 20 min) to remove cell residues. According to the previous protocol, the supernatant after separation was used for the extraction of EPS (Jiang et al. 2020b).

ATR-IR analysis

After dialysis, the extractant was transferred to a centrifuge tube and freeze-dried to complete the EPS extraction for ATR-IR. Finally, protein, polysaccharide, and GSH were extracted from EPS and measured (Jiang et al. 2020b). Attenuated total reflection Fourier transform infrared spectroscopy (ATR-IR) was applied on a Nicolet iS5 Fourier transform infrared spectrometer with Thermo Scientific OMNIC software (Thermo Fisher Scientific Inc., Madison, USA). The spectral region of 800–2000 cm^{-1} was scanned 16 times for each sample at a spectral resolution of 4 cm^{-1}.

Electrochemical characteristics of Rho after Cu^{2+} adsorption

A CHI 660D electrochemical workstation (Shanghai Chenhua Instrument Inc., China) was used to carry out cyclic voltammetry (CV) of Rho before and after Cu^{2+} adsorption. CV is a three-electrode system consisted of a platinum wire auxiliary electrode, a saturated calomel reference electrode (SCE), and the modified glassy carbon electrode (GCE) working electrode.

For fabrication of the aptasensor, the GCE (glassy carbon electrode, 5 mm diameter) was carefully polished by using 0.3 and 0.05 μm of α-Al_2O_3 powder suspension, followed by sonication in ethanol and ultrapure water. After nitrogen

drying, the prepared bare GCE was coated with water dispersed Rho samples (50 μL, 20 mg/mL) and then dried (65 °C, 2 h). 10 μL 0.5 wt% Nafion solution was covered on the above-modified electrode and dried in air. A saturated calomel electrode and a Pt wire were used as reference and counter electrodes, respectively. The electrochemical behaviors were investigated at a scan rate of 10 mV s^{-1} within the scan range from 0.8 to − 0.8 V.

Statistical analysis

SPSS statistical software (v17.0, IBM) was used to analyze the data, and the significance level was $P < 0.05$. The differences between groups are determined by single-factor analysis of variance (Tukey). The data in the figure are the mean of standard deviation ($N = 4$).

Results

Adsorption of Cu and cell counts

The sorption of Cu showed dramatic fluctuation under different degrees of Cu stress. At 50 mg/L Cu^{2+}, the Cu^{2+} removal by Rho was ∼ 35%. At 100 mg/L, the Cu^{2+} removal was lowered to < 10%. At 200 mg/L, no evident sorption was observed, which suggested the weak microbial sorption due to the strong toxicity of Cu^{2+} (Fig. 1A). Cell counts also confirmed the strong Cu^{2+} toxicity to fungal cells. At 0 to 50 mg/L Cu^{2+}, there was a significant decrease in the number of Rho cells from 135 to 60 ($\times 10^9$/50 mL) (Fig. 1B). When the Cu^{2+} concentration increased to 100–200 mg/L level, the cell counts were dramatically declined to 30 and 18 ($\times 10^9$/50 mL) (Fig. 1B).

Measurements of polysaccharides and proteins

The EPS yield was 3328 mg (per L medium) without Cu^{2+} stress (Fig. 2A). When the concentration of Cu^{2+} was 50 mg/L, the EPS yield was slightly elevated to 3550 mg. When the concentrations of Cu^{2+} raised to 100 and 200 mg/L, the EPS production was decreased to 2784 and 2290 mg, respectively. The change of protein within EPS demonstrated a similar trend to that of EPS. The protein content was 53 mg (per g EPS, extracted from the surviving Rho) without Cu^{2+} stress (Fig. 2B). At the Cu^{2+} level of 50 mg/L, the protein concentration (per g EPS) was significantly elevated to 96 mg (Fig. 2B). At 100 mg/L, the concentration decreased to 81 mg. At 200 mg/L, the abundance decreased to 62 mg, close to that in the treatment with 0 mg/L Cu^{2+}.

GSH was also extracted from EPS and was measured (Fig. 2C). At 0–50 mg/L, the GSH concentrations in EPS (per 10^{10} cells, extracted from the survived Rho) slightly decreased
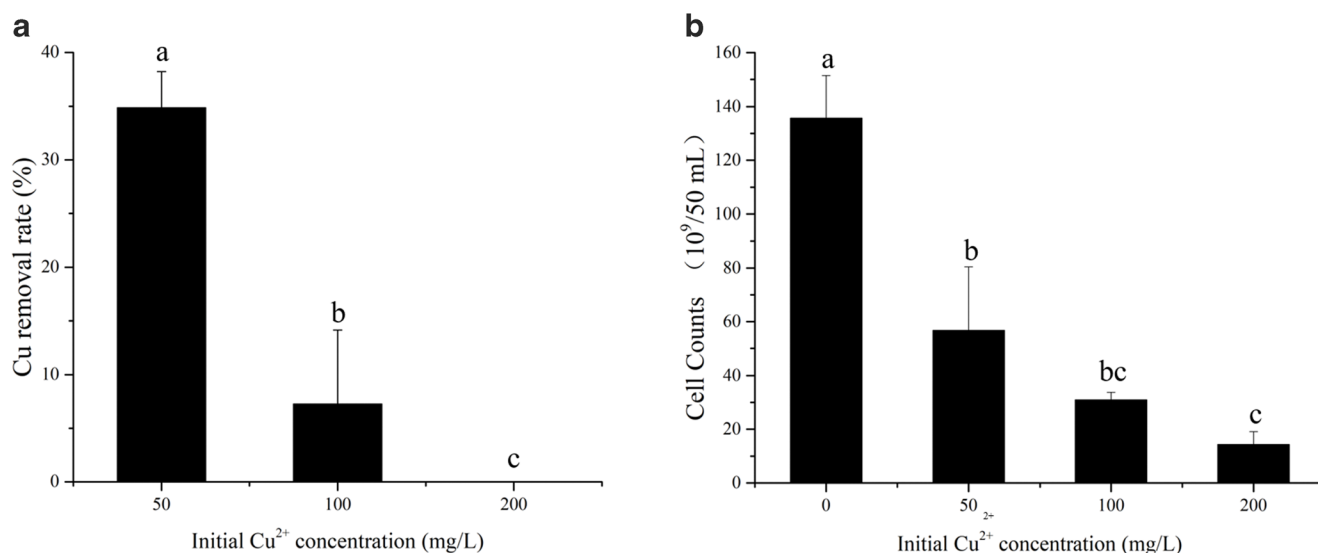
Fig. 1 The removal rate of Cu^{2+} (A) and cell counts of Rho (B) after 72-h incubation at different Cu^{2+} concentrations (0, 50, 100, and 200 mg/L)

from 1.72 to 1.52 nmol, following by a slight increase of GSH to 1.88 nmol at 100 mg/L. Then, at 200 mg/L Cu, there was a markable increase of GSH at 7.62 nmol. However, this value might be virtually enlarged due to the debris of the dead cells, because the standard error is as high as 3.93. The content of polysaccharides from EPS was ~800 mg/g at 0–100 mg/L Cu^{2+} levels (Fig. 2D). However, at 200 mg/L, it dramatically declined to 664 mg (per g EPS) (Fig. 2D). The fluctuation of polysaccharides is also consistent with those of EPS and proteins in EPS.

ATR-IR analysis of EPS

ATR-IR spectra showed multiple characteristic peaks of the extracted Rho EPS after incubation (Fig. 3). The peaks at ~ 1640 and 1730 cm^{-1} are attributed to C=O stretching vibration in carboxyl groups, e.g., -COOH (Mancilla et al. 2009; Wyatt et al. 2013). The C-O-C, C-N, C=O, N-H vibrations are highly related with proteins and saccharides in EPS (Zhang et al. 2018). As the Cu^{2+} increased to 200 mg/L, the peaks of carboxyl (1641 cm^{-1}) and carboxylic acid ester (1727 cm^{-1}) disappeared. Both of the two peaks could be the functional groups of polysaccharides (Gomez-Ordonez and Ruperez 2011). The intensity of the ~ 1640 and 1730 cm^{-1} peak showed an evident decline during the elevation of Cu stress, confirming the Cu toxicity (lower production of organic components). The peaks at 1011 cm^{-1} are usually assigned to the characteristic C-O-C vibration within the sugar ring (Gomez-Ordonez and Ruperez 2011), confirming the abundant polysaccharides in EPS. In addition, the peak at 1238 cm^{-1} is assigned to C-N stretching vibration (Kang et al. 2017). Particularly, the 1541 cm^{-1} peak, which is assigned to the N-H band in amide II component (Jiang et al. 2020b),

disappeared in all the spectra (see Fig. 3). This peak is considered as an indicator of GSH in EPS (Li et al. 2019). Therefore, ATR-IR spectra proved that GSH production did not increase with rising Cu concentrations, which matched the biochemical results in Fig. 2C.

Electrochemical characterization of Rho modified electrodes

The Rho-Cu composite was studied by cyclic voltammetry in PBS buffer (pH = 7.0). At the scanning rate of 10 mV s^{-1}, no significant peak value was observed in the yeast collected from 0 mg/L medium (Fig. 4), indicating that there were few active substances under the oxidation/reduction states. The yeast cells after incubation with 200 mg/L Cu^{2+} (no wash) showed clear redox peaks at − 0.35 V (reduction) and − 0.02 V (oxidation), respectively (Shen et al. 2015). This was corresponding to the reversible valence transition of Cu^{2+}/Cu$^+$. After the removal of labile EPS (after wash), the oxidation peak disappeared. Only a weak reduction peak (− 0.35 V) appeared, indicating the presence of sole and low reducing active substances.

Cell morphology under transmitted electron microscopy

At the millimeter scale, the integrity of the capsule was gradually degraded with the increasing Cu^{2+} concentrations. At 50 mg/L, only a few cells lost its membrane integrity (see the boxed cell in Fig. 5A). The primary damage was evidently observed on the cell membrane (see the downright corner in Fig. 5B). The thickness of the cell membrane was ~450 nm and the sizes of the typical large Ves under transmission
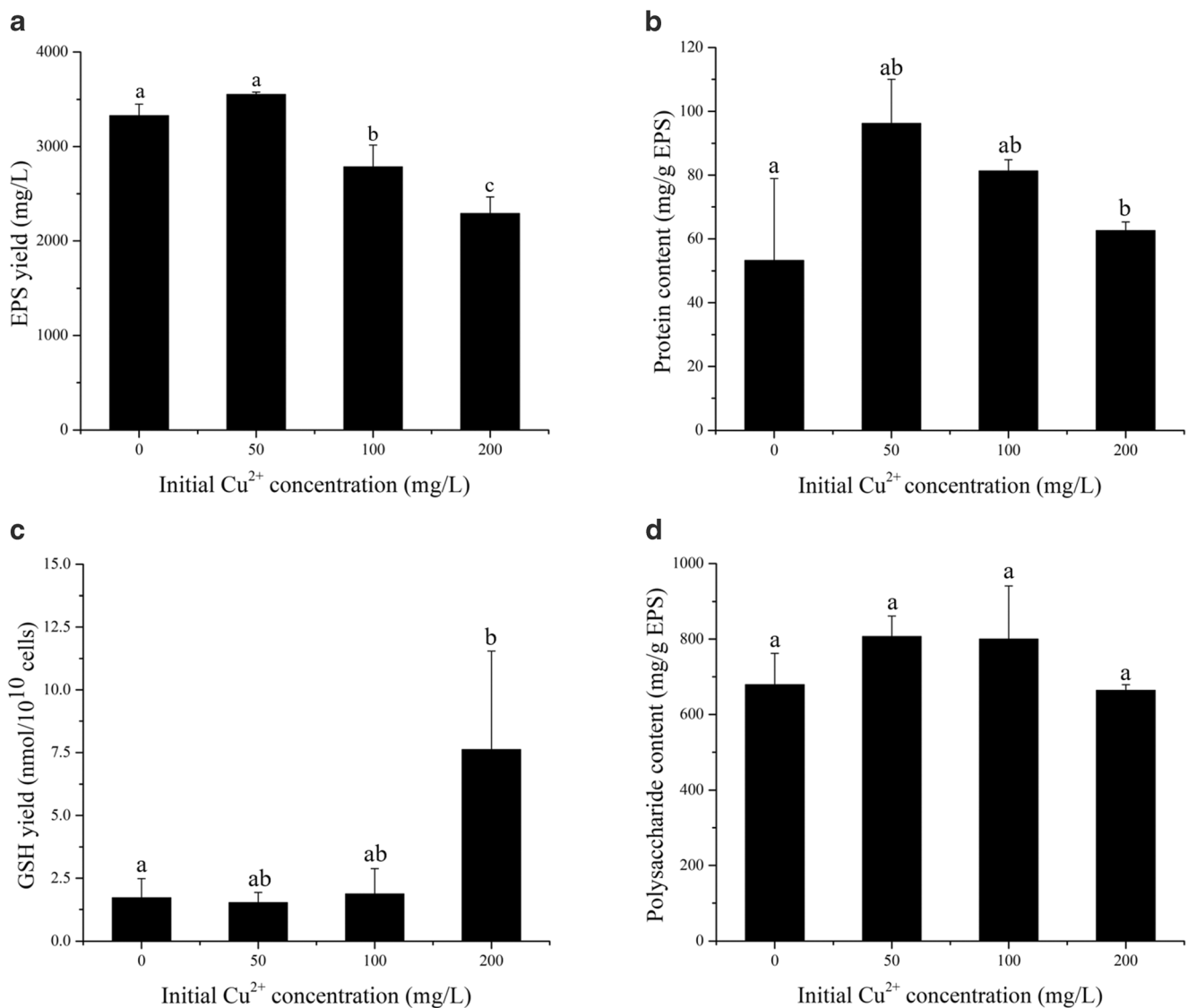
Fig. 2 The yields of EPS (A), proteins (per g EPS) (B), GSH (per 1010 cells) (C), and polysaccharides (per g EPS) (D) after 72-h incubation at different Cu^{2+} concentrations (0, 50, 100, and 200 mg/L)

electron microscopy (TEM) were 330–400 nm (diameter). At 100 mg/L, more cells were deformed (Fig. 5C, D). Their cell membrane had completely lost its integrity; i.e., the membrane is not as smooth as usual. The Ves diameter and number of the cells of 100 mg/L are significantly larger than those of 50 mg/L treatment, whereas the thickness of the membrane decreased to ~ 315 nm. At 200 mg/L, the cells were further distorted and the cytoplasm was unclear under TEM (Fig. 5E, F). It was also difficult to identify the Ves with regular shape. Moreover, both the thickness of membrane and cell size showed evident decline, i.e., down to 116 nm and 2510 nm respectively.

In the unstained sections (exclude the influences of Pb/U particles), it showed that excessive Cu nanoparticles transported into the cell membranes (Fig. 6A, B). TEM images indicated that metal particles were distributed on the surface of the intracellular Ves (see the circled area in Fig. 6B).

At 200 mg/L Cu^{2+} (Fig. 6C, D), the Ves of the cells were obviously deformed; e.g., the edge of the cells was more irregular. These evidences were consistent with the results from the above Fig. 5E, F. Meanwhile, as the rising Cu^{2+} concentration, Cu was adsorbed onto the intracellular Ves (see the circled area in Fig. 6D). The sorption of heavy metals on the cell membrane can be clearly observed under TEM (Jiang et al. 2020a). However, there was no identifiable sorption of Cu nanoparticles on Rho membrane (Fig. 6A, C).

Discussion

Both extra- and intracellular pathways contribute to the detoxification of Cu^{2+} in Rho. EPS are considered as critical extracellular zones to shield the cells against heavy metal stress.
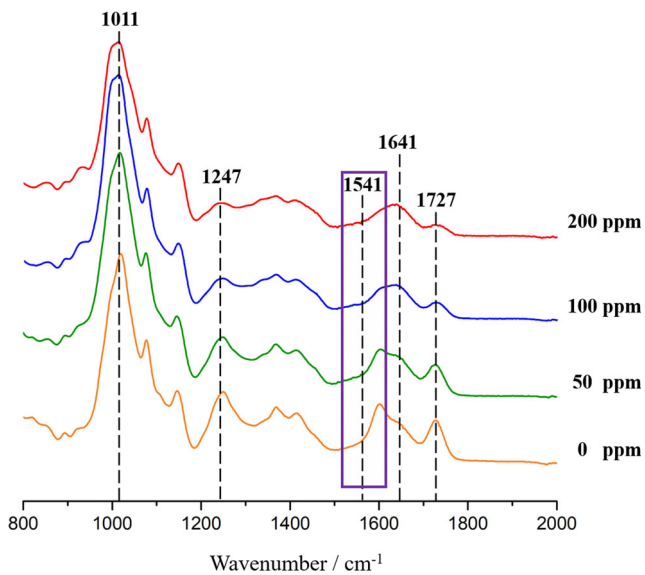
Fig. 3 ATR-IR spectra of the extracted EPS from Rho after incubation at different Cu^{2+} concentrations (0, 50, 100, and 200 mg/L)

However, EPS might have limited ability to resist Cu^{2+} toxicity, especially under high Cu stress. Based on our results, Rho maintained its ability regarding the production of EPS when $Cu^{2+} < 100$ mg/L (see Fig. 2A). However, when the concentration of Cu^{2+} arrived at 200 mg/L, the number of cells and the EPS show a significant downward trend (Fig. 1B and Fig. 2A). Meanwhile, the removal rates of Cu^{2+} were almost under the detection limit (Fig. 1A). Due to the destruction of EPS structure by Cu^{2+}, the cells would have higher possibility to be exposed to the Cu^{2+} stress (Sheng et al. 2013). Additionally, without EPS adsorption, the low removal rate of Cu^{2+} further enhanced the contrast of cations concentration inside/outside Rho cells, enlarging the permeability of Cu^{2+}. The shrinkage
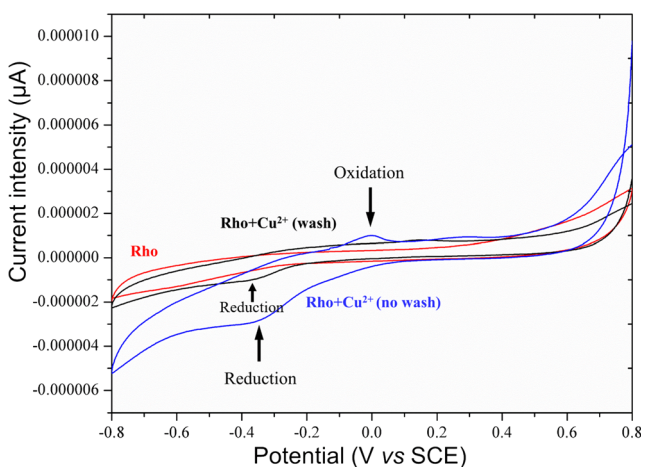

Fig. 4 Electrochemical analysis of Rho cells collected from the treatments with no Cu stress and 200 mg/L Cu^{2+} incubation. For the Rho cells collected after incubated at 200 mg/L Cu^{2+}, part of the dried cells was also washed to remove labile EPS for comparison

of the cells under TEM during the raising Cu levels also confirmed this rising contrast between extracellular and intracellular region (due to the efflux of cell fluid to the region with high ion concentration). Both the enhanced exposure and ion concentration differences led to the continuous high Cu toxicity to Rho cells.

Formation of GSH-heavy metal complex is an important pathway during detoxification. Many heavy metals can induce GSH synthesis to a certain extent in microorganisms, alleviating the oxidative damage (Luna et al. 1994). However, we observed that the content of GSH remained almost unchanged under the stimulation of Cu^{2+}. It may be due to that high concentration of heavy metal cations can inhibit glutathione reductases (GR) activity (Canesi et al. 1999). This is different from the pathways for many other heavy metal cations. For example, the contents of GSH from EPS are enhanced under stress of Pb^{2+}, Hg^{2+}, and Zn^{2+} (Canesi et al. 1999; Li et al. 2019). It is possible that these heavy metals own a lower rate of oxidation process compared with Cu (Liu et al. 2014a). Only Cd^{2+} shows similar strong toxicity to GSH. Therefore, as well as Cd, the declined GSH could be due to that the GSH formed by L-glutathione oxidized cannot make up for the GSH consumed by detoxification (Swiergosz-Kowalewska et al. 2006).

Redox reactions can appear in both extracellular and intracellular regions under Cu^{2+} stress. Rho showed a reversible valence changing from Cu^{2+} to Cu^+, which may be related to the oxidative function of yeast secretion in vitro (Bishop et al. 2007). Cu^{2+} complexed with EPS may undergo reversible valence conversion between Cu^{2+}/Cu^+. Both oxidation and reduction reactions were identified in EPS (see the contrast between wash/no-wash treatments in Fig. 4). Cu^{2+} can interact with free radicals (especially oxygen), then generate reactive oxygen species (ROS) (including O_2^-, H_2O_2, and OH) to cause toxicity to microorganisms (Eqs. 1 and 2). Haber-Weiss reaction produces highly active ·OH (Eq. 2), which is extremely toxic:

$$O2^- + Cu2 + \rightarrow O2 + Cu+ \quad (1)$$

$$Cu + + H2O2 \rightarrow Cu2 + + OH^- + \cdot OH \quad (2)$$
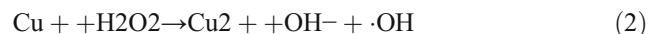
Then, the strong cytotoxic effect of Cu^{2+} in this study may be due to the formation of excessive free radicals in the cells through repeated oxidation cycle, causing substantial damages to mitochondrial lipid peroxidation and DNA (Gaetke and Chow 2003). To the contrast, the weak toxicity of Pb to yeast cells (based on our previous study) (Jiang et al. 2020b) may be related to the disability of Pb to generate ·OH in cells through Haber-Weiss reaction. It should also be addressed that the Haber-Weiss reaction can also occur in intracellular region, as well as in EPS. However, after removal of labile EPS, the weak reduction intensity and the disappeared oxidation signal
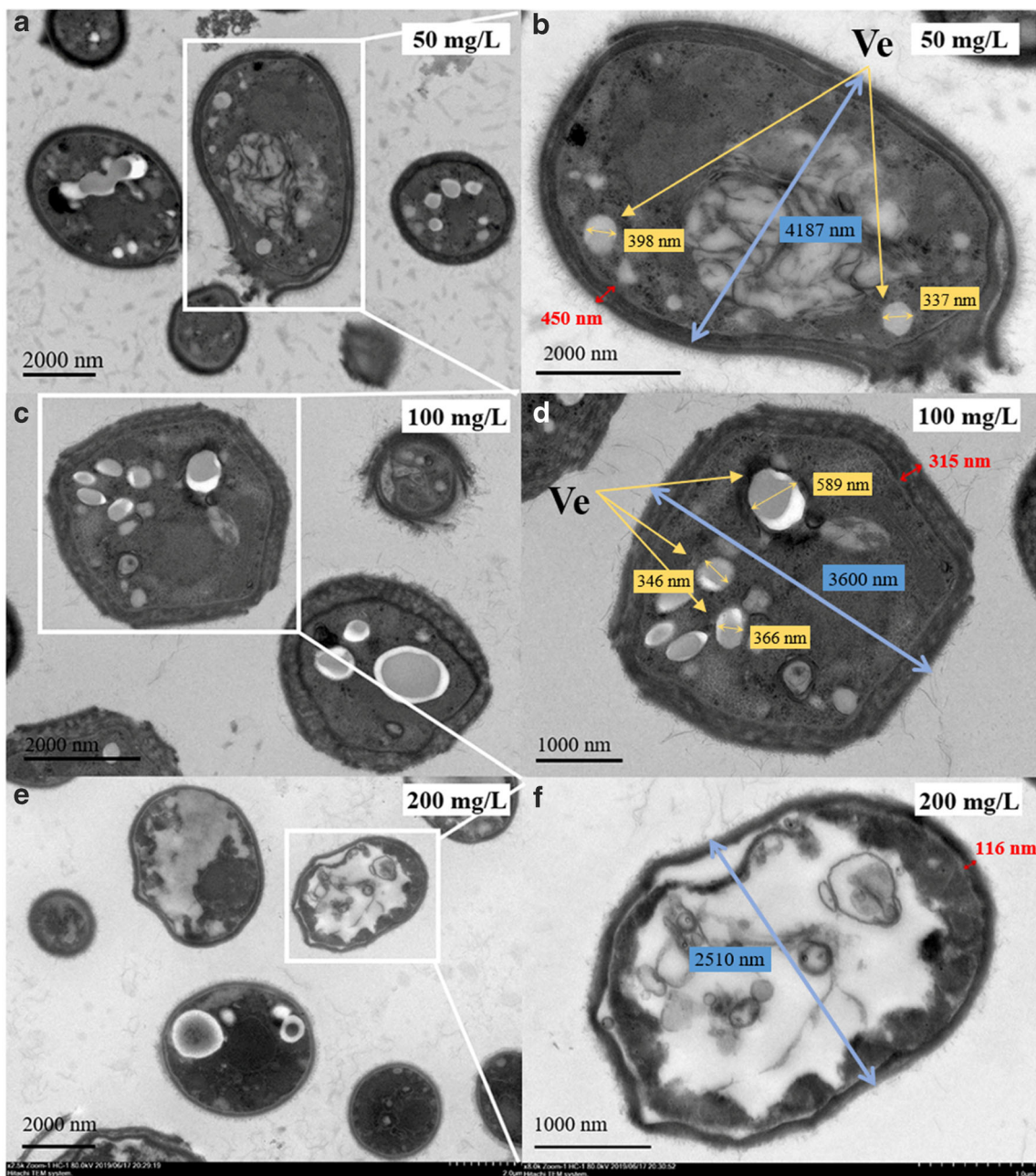
Fig. 5 Transmission electron microscope (TEM) imaging on the Rho sections (stained) after 72-h incubation at Cu^{2+} levels of 50 (A and B), 100 (C and D) and 200 (E and F) mg/L

suggested the limited possibility of intracellular redox reaction under Cu stress.

The cell membrane did not show the high ability to absorb Cu cations as confirmed by Cu nanoparticles on cell membrane (Fig. 6). The cell membrane thickness treated with 200 mg/L Cu^{2+} was only 1/4 of that exposed to 0 mg/L Cu^{2+}. Meanwhile, the membrane is more irregular and no evident metal nanoparticles (usually is dark under TEM due to the high atomic weight) were observed in the unstained section (see Fig. 6C). These morphological changes of cell membrane may be related to the conformational changes of phospholipid molecules in cell membrane (Suwalsky et al. 1998). In addition, the increased contrast of extracellular and intracellular ion concentrations may also lead to these deformations. These phenomena will degrade the function of membrane to shield against Cu cations, whereas the penetration of Cu into cells will be enhanced. Furthermore, after EPS removal, the peak values of redox and oxidation states were decreased or even disappeared, indicating that the redox reaction on the cell membrane was weak (Fig. 4).
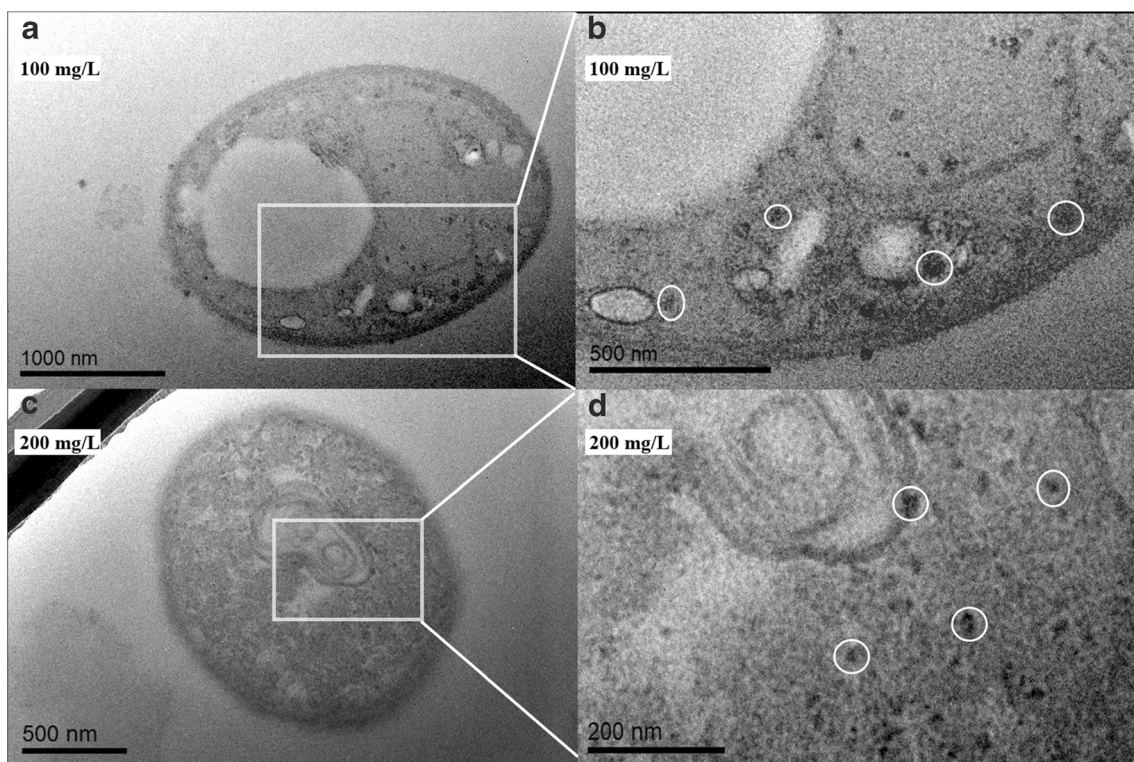
Fig. 6 Transmission electron microscope (TEM) images of Rho sections (unstained) after 72-h incubation at Cu^{2+} levels of 100 (A and B) and 200 (C and D) mg/L

Ves is the primary component in intracellular detoxification (Jiang et al. 2020b). Previous studies demonstrated that Cu cations can be transported from the cytoplasm to Ves by metal carriers located on their membrane. Heavy metal transporters and metal chelating proteins in Ves can be stored via binding to metal cations (Miyayama et al. 2009; Nevitt et al. 2012). At 100 mg/L, a large number of Cu cations were observed on the Ves (Fig. 6), which confirmed that the cells are still functional. TEM results also indicated a significant increase in the number and size of Ves with increasing Cu^{2+} concentration, which confirmed that the ability of intracellular Ves to transport Cu cations was activated. However, the shapes of the Ves were tortured under 200 mg/L Cu^{2+} stress (see Fig. 5F). Then, the detoxification by Ves would be significantly weakened. Therefore, Ves have limited ability to assist the efflux of Cu, which is different from other heavy metals, e.g., Ves own high ability to transport Pb cations under up to 2500 mg/L Pb^{2+} stress (Jiang et al. 2020b).

EPS and intracellular Ves are functional in Cu detoxification as Cu < 100 mg/L. However, the production of EPS and the transportation of Ves were significantly inhibited when Cu^{2+} level over 100 mg/L in Rho, which greatly reduced the ability of Cu detoxification for fungal cells. Meanwhile, the deformation of the cell membrane caused its weakened sorption of Cu nanoparticles. We proposed that EPS cannot bind to abundant Cu cations, which accelerates the penetration of Cu into intracellular region. The redox reaction in EPS further increases Cu toxicity. Then, the contrast of Cu concentration between extracellular and intracellular is enlarged. Finally, the degraded cell membrane and Ves enhanced Cu toxicity.

Code availability Not applicable.

Authors' contributions W.M.X. conceived and designed the study. M.J.X. and W.X.W carried out experiments and analyzed the data. L.Z. and C.H.M. improved the experiment and provided experimental resources. W.Z.J. and T.L.Y. contributed new reagents and analytical tools. W.M.X., M.J.X., and W.X.W. wrote the manuscript. L.Z. and C.H.M. suggested revisions to the manuscript. All the authors read and approved the manuscript.

Data availability The data and material are real, available, and transparent.

Compliance with ethical standards

Conflict of interest The authors declare that they have no conflict of interest.

Ethical approval This article does not contain any studies with human participants or animals performed by any of the authors.

References

Bishop GM, Dringen R, Robinson SR (2007) Zinc stimulates the production of toxic reactive oxygen species (ROS) and inhibits glutathione reductase in astrocytes. Free Radic Biol Med 42(8):1222–1230. https://doi.org/10.1016/j.freeradbiomed.2007.01.022

Bondarczuk K, Piotrowska-Seget Z (2013) Molecular basis of active copper resistance mechanisms in Gram-negative bacteria. Cell Biol Toxicol 29(6):397–405. https://doi.org/10.1007/s10565-013-9262-1

Bulcke F, Santofimia-Castano P, Gonzalez-Mateos A, Dringen R (2015) Modulation of copper accumulation and copper-induced toxicity by antioxidants and copper chelators in cultured primary brain astrocytes. J Trace Elem Med Biol 32:168–176. https://doi.org/10.1016/j.jtemb.2015.07.001

Canesi L, Viarengo A, Leonzio C, Filippelli M, Gallo G (1999) Heavy metals and glutathione metabolism in mussel tissues. Aquat Toxicol 46(1):67–76. https://doi.org/10.1016/s0166-445x(98)00116-7

Cervantes C, Gutierrezcorona F (1994) Copper resistance mechanisms in bacteria and fungi. FEMS Microbiol Rev 14(2):121–137. https://doi.org/10.1016/0168-6445(94)90002-7

Eisses JF, Chi Y, Kaplan JH (2005) Stable plasma membrane levels of hCTR1 mediate cellular copper uptake. J Biol Chem 280(10):9635–9639. https://doi.org/10.1074/jbc.M500116200

Gaetke LM, Chow CK (2003) Copper toxicity, oxidative stress, and antioxidant nutrients. Toxicology 189(1–2):147–163. https://doi.org/10.1016/s0300-483x(03)00159-8

Gomez-Ordonez E, Ruperez P (2011) FTIR-ATR spectroscopy as a tool for polysaccharide identification in edible brown and red seaweeds. Food Hydrocoll 25(6):1514–1520. https://doi.org/10.1016/j.foodhyd.2011.02.009

Gorobets S, Gorobets O, Ukrainetz A, Kasatkina T, Goyko I (2004) Intensification of the process of sorption of copper ions by yeast of *Saccharomyces cerevisiae* 1968 by means of a permanent magnetic field. J Magn Magn Mater 272:2413–2414. https://doi.org/10.1016/j.jmmm.2003.12.840

Gouva E (2020) Reduced metabolic rate and increased heart beat as early signs of sub lethal copper toxicity in developing zebrafish. Asian J Agri Biol 8:119–128. https://doi.org/10.35495/ajab.2019.09.415

Harish R, Samuel J, Mishra R, Chandrasekaran N, Mukherjee A (2012) Bio-reduction of Cr(VI) by exopolysaccharides (EPS) from indigenous bacterial species of Sukinda chromite mine, India. Biodegradation 23(4):487–496. https://doi.org/10.1007/s10532-011-9527-4

Jiang ZQ, Jiang L, Zhang L, Su M, Tian D, Wang T, Sun YL, Nong Y, Hu SJ, Wang SM, Li Z (2020a) Contrasting the Pb (II) and Cd (II) tolerance of *Enterobacter* sp. via its cellular stress responses. Environ Microbiol 22(4):1507–1516. https://doi.org/10.1111/1462-2920.14719

Jiang ZQ, Wang T, Sun YL, Nong Y, Tang LY, Gu TT, Wang SM, Li Z (2020b) Application of Pb(II) to probe the physiological responses of fungal intracellular vesicles. Ecotoxicol Environ Saf 194:8. https://doi.org/10.1016/j.ecoenv.2020.110441

Kan G, Wang X, Jiang J, Zhang C, Chi M, Ju Y, Shi C (2019) Copper stress response in yeast *Rhodotorula mucilaginosa* AN5 isolated from sea ice, Antarctic. Microbiol Open 8:657. https://doi.org/10.1002/mbo3.657

Kang FX, Qu XL, Alvarez PJJ, Zhu DQ (2017) Extracellular saccharide-mediated reduction of Au^{3+} to gold nanoparticles: new insights for heavy metals biomineralization on microbial surfaces. Environ Sci Technol 51(5):2776–2785. https://doi.org/10.1021/acs.est.6b05930

Kaplan M (1999) Accumulation of copper in soils and leaves of tomato plants in greenhouses in Turkey. J Plant Nutr 22(2):237–244. https://doi.org/10.1080/01904169909365622

Kenney J, Fein J (2011) Importance of extracellular polysaccharides on proton and Cd binding to bacterial biomass: a comparative study. Chem Geol 286:109–117. https://doi.org/10.1016/j.chemgeo.2011.04.011

Li J, Jiang Z, Chen S, Wang T, Jiang L, Wang M, Wang S, Li Z (2019) Biochemical changes of polysaccharides and proteins within EPS under Pb (II) stress in *Rhodotorula mucilaginosa*. Ecotoxicol Environ Saf 174:484–490. https://doi.org/10.1016/j.ecoenv.2019.03.004

Liu J, Liu H, Li Y, Wang H (2014a) Probing the coordination properties of glutathione with transition metal ions ($Cr^{2+}, Mn^{2+}, Fe^{2+}, Co^{2+}, Ni^{2+}, Cu^{2+}, Zn^{2+}, Cd^{2+}, Hg^{2+}$) by density functional theory. J Biol Phys 40(4):313–323. https://doi.org/10.1007/s10867-014-9350-3

Liu T, Li F, Zhang X, Zhang H, Duan D, Shen C, Hashmi MZ, Shi J (2014b) Tracing intracellular localization and chemical forms of copper in Elsholtzia splendens with cluster analysis. Biol Trace Elem Res 160(3):418–426. https://doi.org/10.1007/s12011-014-0043-3

Luna CM, Gonzalez CA, Trippi VS (1994) Oxidative damage caused by an excess of copper in oat leaves. Plant Cell Physiol 35(1):11–15. https://doi.org/10.1093/oxfordjournals.pcp.a078561

Mancilla N, D'Antonio MC, Gonzalez-Baro AC, Baran EJ (2009) Vibrational spectra of lead(II) oxalate. J Raman Spectrosc 40(12):2050–2052. https://doi.org/10.1002/jrs.2370

Miyayama T, Suzuki KT, Ogra Y (2009) Copper accumulation and compartmentalization in mouse fibroblast lacking metallothionein and copper chaperone, Atox1. Toxicol Appl Pharmacol 237(2):205–213. https://doi.org/10.1016/j.taap.2009.03.024

Nevitt T, Ohrvik H, Thiele DJ (2012) Charting the travels of copper in eukaryotes from yeast to mammals. Biochim Biophys Acta, Mol Cell Res 1823(9):1580–1593. https://doi.org/10.1016/j.bbamcr.2012.02.011

Pearce DA, Sherman F (1999) Toxicity of copper, cobalt, and nickel salts is dependent on histidine metabolism in the yeast *Saccharomyces cerevisiae*. J Bacteriol 181(16):4774–4779. https://doi.org/10.1128/JB.181.16.4774-4779.1999

Podanyi B, Reid R (1988) NMR study of the conformations of free and lanthanide-complexed glutathione in aqueous solution. J Am Chem Soc 14:110. https://doi.org/10.1021/ja00220a014

Quigley MS, Santschi PH, Hung CC, Guo LD, Honeyman BD (2002) Importance of acid polysaccharides for Th-234 complexation to marine organic matter. Limnol Oceanogr 47(2):367–377. https://doi.org/10.4319/lo.2002.47.2.0367

Ramsay LM, Gadd GM (1997) Mutants of *Saccharomyces cerevisiae* defective in vacuolar function confirm a role for the vacuole in toxic metal ion detoxification. FEMS Microbiol Lett 152(2):293–298. https://doi.org/10.1111/j.1574-6968.1997.tb10442.x

Rehman M, Liu L, Wang Q, Saleem MH, Bashir S, Ullah S, Peng D (2019) Copper environmental toxicology, recent advances, and future outlook: a review. Environ Sci Pollut Res 26(18):18003–18016. https://doi.org/10.1007/s11356-019-05073-6

Sakhaee E, Kazeminia S (2011) Relationship between liver and blood plasma copper level and abortion in cattle. Comp Clin Pathol 20(5):467–469. https://doi.org/10.1007/s00580-010-1020-7

Shen W-J, Zhuo Y, Chai Y-Q, Yuan R (2015) Cu-based metal–organic frameworks as a catalyst to construct a ratiometric electrochemical aptasensor for sensitive lipopolysaccharide detection. Anal Chem 87(22):11345–11352. https://doi.org/10.1021/acs.analchem.5b02694

Sheng GP, Xu J, Luo HW, Li WW, Li WH, Yu HQ, Xie Z, Wei SQ, Hu FC (2013) Thermodynamic analysis on the binding of heavy metals onto extracellular polymeric substances (EPS) of activated sludge.

Water Res 47(2):607–614. https://doi.org/10.1016/j.watres.2012.10.037

Silver S, Walderhaug M (1992) Gene-regulation of plasmid-determined and chromosome-deter-mined inorganic-ion transport in bacteria. Microbiol Rev 56(1):195–228. https://doi.org/10.1128/MMBR.56.1.195-228.1992

Solioz M, Abicht HK, Mermod M, Mancini S (2010) Response of gram-positive bacteria to copper stress. J Biol Inorg Chem 15(1):3–14. https://doi.org/10.1007/s00775-009-0588-3

Suwalsky M, Ungerer B, Quevedo L, Aguilar F, Sotomayor CP (1998) Cu^{2+} ions interact with cell membranes. J Inorg Biochem 70(3–4):233–238. https://doi.org/10.1016/s0162-0134(98)10021-1

Swiergosz-Kowalewska R, Bednarska A, Kafel A (2006) Glutathione levels and enzyme activity in the tissues of bank vole clethrionomys glareolus chronically exposed to a mixture of metal contaminants. Chemosphere 65(6):963–974. https://doi.org/10.1016/j.chemosphere.2006.03.040

Tian D, Li Z, O'Connor D, Shen ZT (2020) The need to prioritize sustainable phosphate-based fertilizers. Soil Use Manag 36(3):351–354. https://doi.org/10.1111/sum.12578

Wang JL (2002) Biosorption of copper(II) by chemically modified biomass of *Saccharomyces cerevisiae*. Process Biochem 37(8):847–850. https://doi.org/10.1016/s0032-9592(01)00284-9

Wang YY, Qin J, Zhou S, Lin XM, Ye L, Song CK, Yan Y (2015) Identification of the function of extracellular polymeric substances (EPS) in denitrifying phosphorus removal sludge in the presence of copper ion. Water Res 73:252–264. https://doi.org/10.1016/j.watres.2015.01.034

Wei LL, Li Y, Noguera DR, Zhao NB, Song Y, Ding J, Zhao QL, Cui FY (2017) Adsorption of Cu^{2+} and Zn^{2+} by extracellular polymeric substances (EPS) in different sludges: effect of EPS fractional polarity on binding mechanism. J Hazard Mater 321:473–483. https://doi.org/10.1016/j.jhazmat.2016.05.016

Wyatt VT, Yadav MP, Latona N, Liu CK (2013) Thermal and mechanical properties of glycerol-based polymer films infused with plant cell wall polysaccharidese. J Biobased Mater Bioenergy 7(3):348–356. https://doi.org/10.1166/jbmb.2013.1368

Yadav SK (2010) Heavy metals toxicity in plants: an overview on the role of glutathione and phytochelatins in heavy metal stress tolerance of plants. S Afr J Bot 76(2):167–179. https://doi.org/10.1016/j.sajb.2009.10.007

Zhang XY, Zhang L, Zou X, Han FY, Yan ZP, Li Z, Hu SJ (2018) Semi-quantitative analysis of microbial production of oxalic acid by montmorillonite sorption and ATR-IR. Appl Clay Sci 162:518–523. https://doi.org/10.1016/j.clay.2018.07.006